Pharmaceutical Sciences Asia

Pharm Sci Asia 2026; 53(2), 146-156

DOI:10.29090/psa.2026.02.26.9290

Research Article

Hair regrowth effects of ethyl acetate extract from *Perilla frutescens* leaves combined with LED photobiomodulation in a testosterone-induced alopecia mouse model

Nguyen Anh Thu Le[1+], Do Hoang Vy Nguyen[1+], Truong Giang Tran[1], Thi Thu Hien Pham[2], Ngoc Trinh Huynh[1*]

[1] School of Pharmacy, University of Medicine and Pharmacy at Ho Chi Minh City, Ho Chi Minh city, VietNam
[2] School of Biomedical Engineering, International University, Ho Chi Minh City, VietNam

ABSTRACT

Androgenetic alopecia (AGA) is the most common form of hair loss, affecting nearly 50% of adults by midlife. This study investigated the therapeutic potential of an ethyl acetate (EA) extract from *Perilla frutescens* leaves, light-emitting diode (LED) therapy, and their combination in a testosterone-induced AGA mouse model. Male Swiss *albino* mice received subcutaneous testosterone (1.0 mg/day, 5 days/week) to induce AGA and were treated topically with 2% minoxidil, 5% EA extract, LED therapy (655 ± 5 nm, 20 min every two days), or the EA+LED combination. Untreated AGA mice received testosterone and 5% glycerin, while physiological controls received sesame oil and glycerin. Hair regrowth was assessed by macroscopic scoring, follicle quantification and histological evaluation of hair-cycle stages. Physiological group achieved full macroscopic regrowth by Day 31, whereas untreated mice showed progressive deterioration. EA and LED monotherapies significantly improved follicle preservation and hair cycle progression, with LED therapy effectively supporting anagen advancement. The combination therapy produced the most pronounced effects, achieving near-complete regrowth by Day 35 along with the highest follicle density and anagen/telogen ratio. Histological analysis confirmed marked dermal and follicular restoration. These findings indicate that EA extract combined with LED therapy markedly enhances hair regrowth efficacy in AGA.

Keywords:
Androgenetic alopecia; Hair regrowth; LED photobiomodulation; *Perilla frutescens*

1. INTRODUCTION

Androgenetic alopecia (AGA), commonly referred to as male or female pattern baldness, represents the most prevalent form of hair loss, affecting approximately 50% of both men and women by the age of 50 [1]. The psychological burden associated with AGA is substantial, often manifesting as diminished self-esteem, negative body image, and social anxiety. The pathogenesis of AGA is primarily attributed to dihydrotestosterone (DHT), a potent androgen derived from testosterone via the enzymatic activity of 5α-reductase type 2 within hair follicle tissues [2,3]. DHT binds to androgen receptors in hair follicles, leading to a shortened anagen phase and a premature transition to the telogen phase, thereby impairing the follicle's capacity to produce terminal hair. Clinically, AGA is characterized by progressive follicular miniaturization, resulting in thinner hair shafts and reduced hair density.

***Corresponding author:**
* Ngoc Trinh Huynh Email: hntrinh@ump.edu.vn
+Contributed equally:
+ Nguyen Anh Thu Le, Do Hoang Vy Nguyen

Currently, the U.S. Food and Drug Administration (FDA) has approved topical minoxidil and oral finasteride as therapeutic agents for AGA. While these treatments can decelerate hair loss and stimulate regrowth, their use is frequently limited by adverse effects and variable patient responsiveness [4-6].

Perilla frutescens L. is a widely cultivated vegetable and medicinal herb in several Asian countries including China, Japan, Korea and Vietnam. Various parts of the plant, particularly the leaves and seeds, are rich in a diverse spectrum of bioactive compounds, notably linoleic acid, rosmarinic acid, luteolin, and catechin [7,8]. These phytochemicals possess well-documented pharmacological activities, including antioxidant, anti-inflammatory, and anti-allergic effects. Recent studies have highlighted the potential of *Perilla frutescens* leaf extract in promoting hair growth. The n-butanol fraction from *Perilla frutescens* leaves stimulated proliferation and differentiation of hair follicle matrix cells, thereby prolonging the anagen phase [9]. Additionally, rosmarinic acid, one of the major constituents isolated from Perilla, has demonstrated hair growth-enhancing properties through mechanisms associated with follicular activation and regeneration [9]. Furthermore, our previous study reported that a 5% ethanol extract of Perilla leaves effectively promoted hair regrowth in a cyclophosphamide-induced alopecia mouse model [10]. Muangsanguan *et al.* additionally found that germinated Perilla seeds possess elevated levels of bioactive compounds capable of inhibiting 5α-reductase and activating the IGF-1/VEGF signaling pathway, contributing to hair regeneration [11]. Collectively, these findings underscore the therapeutic potential of *Perilla frutescens* in the management of AGA.

Beyond phytotherapeutic approaches, photobiomodulation, particularly low-level light therapy (LLLT), has emerged as a promising non-invasive strategy for the management of various pathological conditions. LLLT has demonstrated therapeutic efficacy in a range of dermatological applications, including wound healing, attenuation of inflammation, and anti-aging effects [12,13]. Increasing evidence also supports its role in hair restoration. Mechanistically, LLLT promotes hair follicle development, prolongs the anagen phase, and enhances the proliferation of dermal papilla cells, thereby contributing to hair regeneration [14,15]. Compared to conventional laser-based systems, light-emitting diodes (LEDs) offer several practical advantages, including lower cost and broader beam coverage, which enable treatment of larger scalp areas [16]. Although LEDs and lasers differ in emission characteristics, both modalities have shown efficacy in stimulating hair growth, particularly within the red-light spectrum ranging from 620 to 750 nm [17]. Optimal treatment parameters typically involve energy densities of approximately 4 J/cm², wavelengths between 630-670 nm, and power outputs of 5 mW/cm², with exposure durations spanning 3 to 20 minutes per session [15,17]. Notably, Hong Jin Joo *et al.* reported that LED irradiation at 660 nm significantly enhanced the proliferation of human dermal papilla cells [18]. However, the efficacy of LED photobiomodulation is highly dependent on the precise calibration of these parameters; insufficient power delivery may result in suboptimal biological responses, whereas excessive exposure could exert inhibitory effects.

Although emerging evidence supports Perilla extract and LED irradiation as individual interventions with hair-regrowth potential, their combined *in vivo* effect has not yet been elucidated. In this study, we examine whether Perilla extract, red LED irradiation, or their concurrent application enhances hair regrowth in a testosterone-induced alopecia model in Swiss *albino* mice. The findings aim to provide preliminary experimental insight into the therapeutic relevance of integrating these two modalities in the context of AGA management.

2. MATERIALS AND METHODS

2.1. Animals

Male Swiss *albino* mice (17-26 grams) were purchased from the Pasteur Institute in Ho Chi Minh City, Vietnam. Before the experiment, the mice were acclimatized to a 12-hour light-dark cycle for 2-3 days. Throughout the period, animals had free access to the pellet diet of the Pasteur Institute in Ho Chi Minh City (Vietnam) and water *ad libitum*. All experimental protocols were approved under the agreement of the Animal Ethics Committee, Nong Lam University, Ho Chi Minh City, Viet Nam (Approval No. NLU-221202). All experiments were performed in accordance with relevant guidelines and regulations.

2.2. Chemicals

Testosterone propionate (25 mg/mL; Tesmon, Tai Yu Chemical & Pharmaceutical Co., Ltd., China), formalin (Xilong, China), sesame oil (Tuong An Co., Viet Nam), and 2% minoxidil solution (Laboratoires Opodex Industrie, France) were utilized in the study.

2.3. Extraction procedure

Dried *Perilla frutescens* leaves (1,000 g) were collected in June from Dong Thap Province, Vietnam. The plant material was subjected to exhaustive percolation using 50% ethanol at room temperature until no further reaction was observed with ferric chloride ($FeCl_3$), indicating the depletion of phenolic compounds.

The resulting extract was filtered and concentrated under reduced pressure, followed by evaporation to obtain a dried ethanol extract (31.34 g), corresponding to a yield of 25.56% (w/w) and a moisture content of 3.21%. The dried ethanol extract was subsequently dissolved in distilled water at a ratio of 1:10 (v/v) and fractionated with ethyl acetate. The ethyl acetate fraction yielded 7.85 g of dried extract, with a yield of 6.58% (w/w) and a moisture content of 0.56%. Quantitative HPLC analysis revealed rosmarinic acid and luteolin contents of 11.29 ± 0.04 and 1.01 ± 0.01 mg/g, respectively. For *in vivo* experimentation, the dried ethyl acetate extract was dispersed in a 5% glycerin solution to achieve a final concentration of 5% (w/v).

2.4. LED system design

A custom-designed LED irradiation system was developed specifically for this study to deliver controlled red-light exposure to the dorsal skin of mice. The apparatus comprised two primary structural components: (1) a detachable cover incorporating the LED light source, and (2) a rectangular base unit (5 x 5 x 12 cm) partitioned into four individual compartments to accommodate individual mice during treatment (Figure 1A). This configuration ensured uniform light distribution across the treatment area while minimizing animal movement during irradiation.

The control system integrated an ESP32 microcontroller, a high-power MOSFET trigger switch drive module, an LCD display, and associated electronic circuitry (Figure 1B). These components enabled precise adjustment of output power, irradiation duration, and channel-specific operation. Real-time system status was displayed via the LCD interface, and the device was programmed to automatically shut off upon completion of the preset exposure time, thereby ensuring consistent dosing and operational safety.

The light source consisted of 16 high-intensity red LED modules with a peak emission wavelength of 655 ± 5 nm, mounted on a 4 x 1W aluminum printed circuit board (Figure 1C). This configuration was selected based on previous studies indicating that wavelengths within the red-light spectrum (620-750 nm) are optimal for stimulating hair follicle activity [17]. At the lowest energy setting (level 230), the system delivered an output power density of approximately 2.20 mW/cm^2, resulting in a cumulative energy dose of 2.5 J/cm^2 per session. These parameters were carefully calibrated to remain within the therapeutic window for photobiomodulation, thereby minimizing the risk of underexposure while avoiding potential inhibitory effects associated with excessive energy delivery.

During the experimental period, LED irradiation was administered every other day, with each session lasting 20 minutes. The treatment protocol consisted of two 10-minute illumination phases separated by a 5-minute rest interval. Mice were individually placed into designated treatment compartments, and the LED cover was positioned to ensure direct and uniform exposure to the dorsal skin surface. The irradiation procedure was standardized across all treated groups to ensure consistency, reproducibility, and controlled dosing conditions.

In summary, LED irradiation was delivered at 655 nm with an irradiance of approximately 2.00 mW/cm², providing a dose of 2.5 J/cm² per 20-minute session administered every two days, resulting in a cumulative exposure of approximately 20-22.5 J/cm² over the 35-day treatment period.

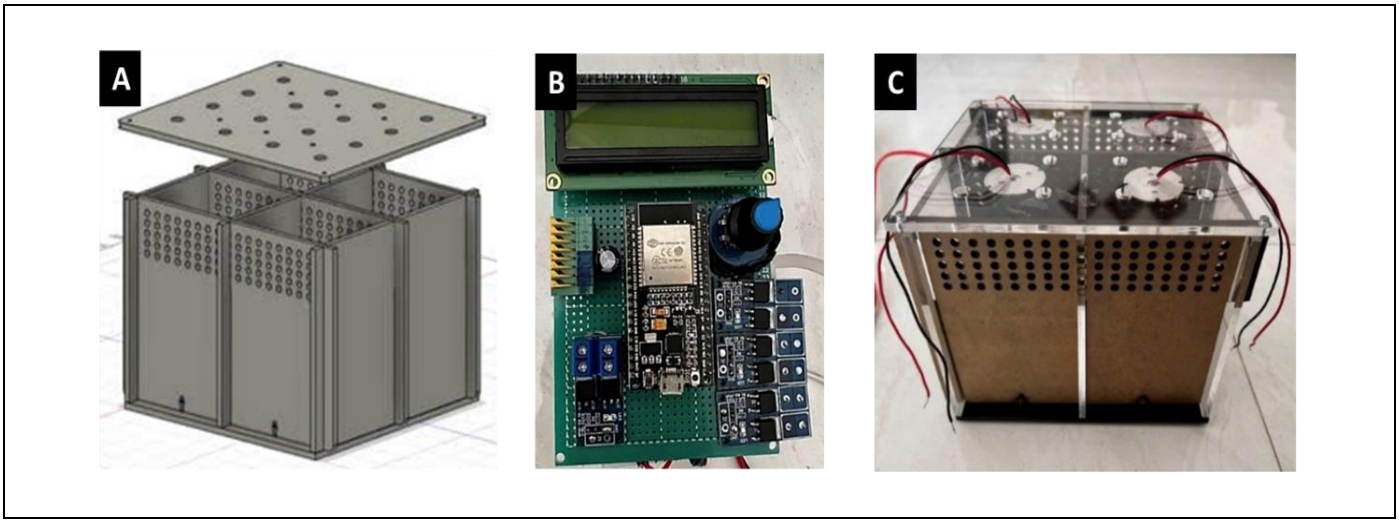

Figure 1. Overview of the custom-designed LED irradiation system. (A) Structural design of the irradiation apparatus comprising a detachable LED cover and a rectangular base unit subdivided into four compartments for animal positioning; (B) Control circuit module incorporating an ESP32 microcontroller, MOSFET driver, and LCD display for precise regulation of irradiation parameters; (C) Assembled device with red LED light source (655 ± 5 nm).

Figure 2. Macroscopic images of hair regrowth evaluated using a 5-point scoring scale.
Scores range from (A) score 0 (no visible hair growth) to score 4 (hair regrowth comparable to unshaved skin).

2.5. Androgen-alopecia induced by testosterone injections

Male Swiss *albino* mice were shaved on the dorsal skin using an electric clipper to create a treatment area measuring approximately 1.5 x 2.5 cm. Three days post-shaving, mice exhibiting no visible hair regrowth or only sparse hair coverage, corresponding to hair growth scores of 0-1 (see Section 2.3), were randomly selected for subsequent experimentation.

Testosterone propionate was dissolved in sesame oil at a concentration of 10 mg/mL. To induce AGA, mice received subcutaneous (SC) injections of 0.1 mL of the testosterone solution, equivalent to a dose of 1.0 mg/day/mouse, administered five consecutive days per week.

2.6. Evaluation of hair regrowth effect

Testosterone-induced alopecia mice were assigned to different experimental groups to evaluate the therapeutic efficacy of various interventions on the shaved dorsal skin:

- Minoxidil group (n=7): topical application of 2% minoxidil once daily.
- EA extract group (n=7): topical application of 5% EA extract once daily.
- LED group (n=8): red-light LED irradiated every other day.
- Combination group (n=8): topical application of 5% EA extract combined with LED irradiation.
- Untreated group (n=7): topical application of 5% glycerin solution only.

Minoxidil, EA extract, and glycerin were applied using a 30 µL micropipette. The solution was gradually dispensed by gently pressing the plunger while rotating the pipette tip over the shaved dorsal skin to ensure uniform distribution. Mice were returned to their cages only after the treated area had completely dried.

Additionally, a physiology group (n=6) was included, in which mice received repeated SC injections of sesame oil (0.1 mL/mouse) and topical application of 5% glycerin solution to the shaved dorsal skin.

The experiment lasted for 35 days. Mice were monitored throughout the study period, and hair-regrowth parameters were recorded at designated time points.

2.6.1. Scoring

Hair regrowth was evaluated macroscopically using a 5-point scale (Figure 2) adapted from previous methods [15], as follows:

- Score 0: no visible hair growth.
- Score 1: sparse, patchy hair growth with visible skin areas.
- Score 2: moderate hair growth; skin remains partially visible.
- Score 3: uniform hair coverage with minimal skin visibility.
- Score 4: hair regrowth in the shaved area comparable to surrounding unshaved regions.

2.6.2. Hair follicle counting

Following macroscopic hair-regrowth scoring, hair removal was performed using an electric clipper on half of the treated dorsal skin area on Day 18 and on the entire treated area at the end of the experiment. Images were randomly acquired from five predefined regions, including four peripheral regions and one central region (Figure 3A). High-resolution images of hair follicles were captured using a 40x macro lens (focal length: 3 cm) attached to a smartphone camera set at 5x magnification, with the lens placed in direct contact with the treated dorsal skin surface (Figure 3B). Subsequently, each image was converted to grayscale to enhance follicle visibility (Figure 3C) and then segmented into eight equal sectors. A hemispherical region comprising four contiguous sectors

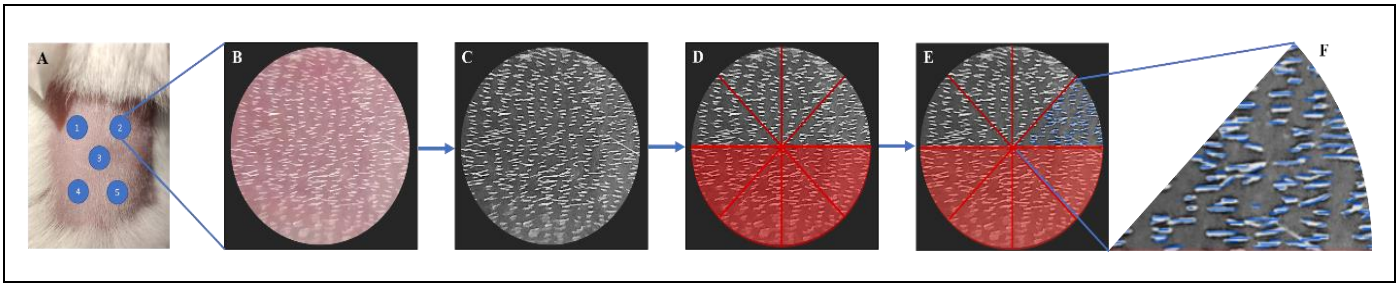

Figure 3. Macroscopic imaging and quantitative assessment of hair follicle counting. (A) Representative image of the treated dorsal skin area indicating five randomly selected imaging regions. (B) High-resolution macroscopic image of hair follicles. (C) Grayscale-converted image used to enhance follicle visibility. (D) Circular image segmented into eight equal sectors; a clearly focused hemispherical region comprising four contiguous sectors was selected for quantification, while the opposite hemisphere exhibiting peripheral blur and optical aberration was excluded (red-shaded area). (E) Manual identification and counting of hair follicles within the selected sectors, with follicles marked in blue. (F) Enlarged view of a representative sector illustrating individual follicle marking.

with high resolution and sharp contrast was selected for primary quantification (Figure 3D), while the opposite hemisphere exhibiting peripheral blur and optical distortion due to lens curvature (optical aberration) was excluded (red-shaded hemisphere). Hair follicles within each selected sector (Figure 3E) were manually counted by marking individual follicles in blue. The total follicle number for each region was extrapolated by doubling the sum obtained from the four contiguous sectors. Finally, the cumulative follicle count from all five regions was used to represent the hair follicle density of the treated dorsal skin area. This assessment was performed on Days 1, 18, and 35 across different experimental groups.

2.6.3. Histological analysis

At the end of the treatment period, animals were euthanized by gradual CO_2 displacement. The treated dorsal skin was excised and fixed in 10% neutral-buffered formalin, followed by paraffin embedding. Longitudinal sections (4-5 µm thick) were prepared and stained with hematoxylin and eosin (H&E). Histological evaluation was performed under a light microscope at 10x magnification. Hair follicles were classified into anagen, catagen, and telogen phases according to established morphological criteria [19,20], as follows:

- Anagen: enlarged follicles extending into the dermis, with complete structures including outer sheath, dermal papilla, inner sheath, hair shaft, and basement membrane.
- Catagen: thickened basement membrane with upward contraction.
- Telogen: wrinkled central core due to keratinization.

The total number of hair follicles and the anagen/telogen ratio were calculated for each experimental group.

2.7. Statistical analysis

Data were compiled and organized using Microsoft Excel 2016. Results are expressed as mean ± SEM (standard error of the mean). Statistical analyses were performed using SPSS version 20.0. Data normality was assessed using the Shapiro-Wilk test. For comparisons between two groups, the independent-samples t-test was applied when data were normally distributed, whereas the Mann-Whitney U test was used for non-normal distributions. Given that six groups were compared in the main analyses, one-way analysis of variance (one-way ANOVA) was used for normally distributed variables, followed by Dunnett's post-hoc multiple comparison test to compare each treatment group with the untreated control. For non-normally distributed variables, the Kruskal-Wallis test followed by Dunn's multiple comparison test was used. Differences in anagen/telogen ratios were evaluated using the Chi-square test. A two-sided p-value < 0.05 was considered statistically significant.

3. RESULTS

3.1. Hair-regrowth score

Hair-regrowth scores increased progressively in all groups throughout the experiment, with significant differences among treatments (Figure 4).

The physiology group exhibited the rapid and sustained improvement, reaching mean scores to 4.0 from Day 31, indicating the complete hair recovery in all mice. In contrast, the untreated group showed minimal improvement, remaining below 2.0 at the endpoint with 11% remaining at score 0-1 and no animals achieving score 4.0 (Figure 5).

Among the treatment groups, the reference treatment by minoxidil induced an early increase in hair growth by Day 5 and rapid increase in hair regrowth scores during the first two weeks, which then gradually plateaued, stabilizing at a mean score of 2-3 by Day 35 (Figure 4). All mice in this group achieved score of 2-3 by Day 35 (Figure 5).

Monotherapy with EA extract or LED irradiation demonstrated gradual improvement and significant gain

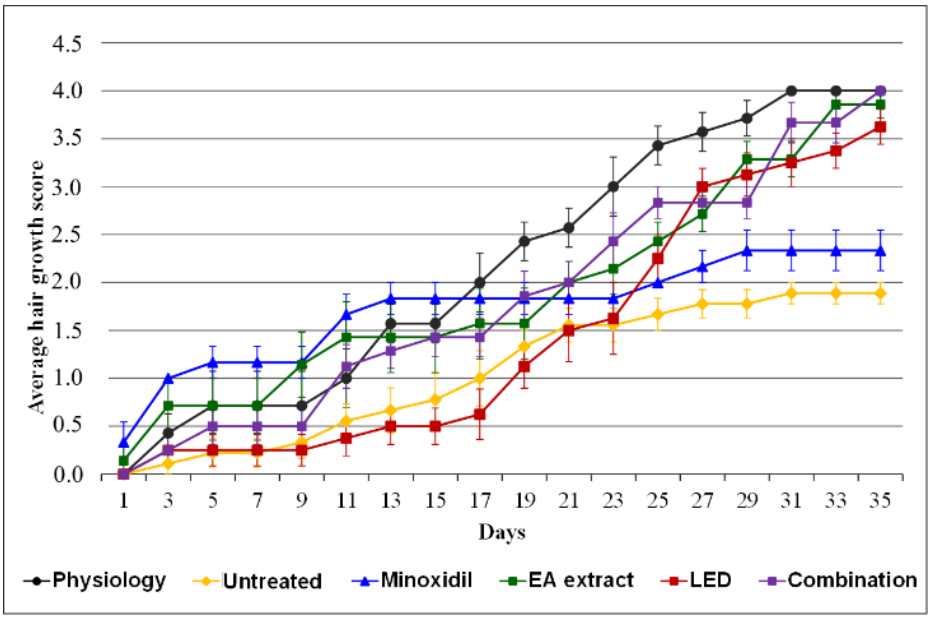

Figure 4. Hair-regrowth scores in experimental groups during the study. Macroscopic hair-regrowth scores were evaluated longitudinally using a 5-point scoring system throughout the experimental period. Data are presented as mean ± SEM.

after day 1, with 86% and 62% of mice reaching score 4, respectively by Day 35. The combination treatment between EA extract and LED irradiation produced a more pronounced overall hair-regrowth response and achieved near-complete hair recovery at the end of the experiment. The combination group exhibited significantly higher hair-regrowth scores than the EA-extract and LED monotherapy groups at specific time points (Days 19, 23, and 25; one-way ANOVA with Dunnett's multiple comparison test; $p < 0.05$), whereas scores were comparable or slightly lower at certain later time points (Days 27, 29, and 33). Despite these temporal variations, the combination treatment resulted in superior hair recovery at the study endpoint. No significant differences were detected between the combination and minoxidil groups at Days 19, 21, and 23; however, the combination group exhibited significantly higher scores than minoxidil from Day 25 through Day 35 ($p < 0.05$).

3.2. Hair follicle count

Normal hair regrowth in the physiology group was characterized by a slight decrease in follicle count by Day 18, followed by a notable increase by Day 35 (Table 1), reflecting the natural regenerative cycle of hair follicles. In contrast, the untreated group exhibited a significant reduction in follicle count at the mid-point of the experiment, with only partial recovery observed by Day 35. Importantly, the follicle counts in the untreated group at both Day 18 and Day 35 were significantly lower than those in the physiology group ($p = 0.000$ and $p = 0.002$, respectively), suggesting that testosterone administration induced progressive follicular degeneration.

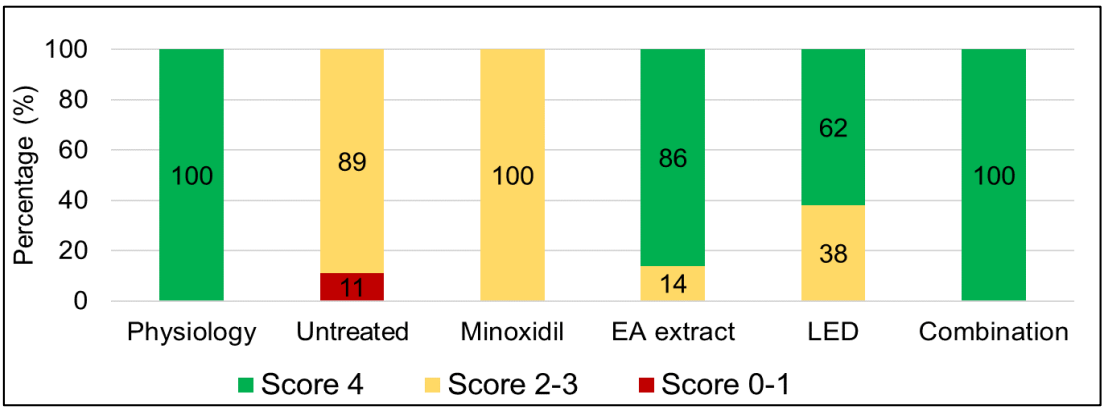

Figure 5. Distribution of hair-regrowth score at the end of the experiment. Stacked bar charts showing the percentage distribution of hair-growth scores (score 0-1, score 2-3, and score 4) in each experimental group on Day 35, based on macroscopic evaluation.

Table 1. The hair follicle counts in each experimental group.

Group	Average counts			% change	
	Day 0	Day 18	Day 35	Day 18	Day 35
Physiology	1995.5 ± 56.7	1971.7 ± 79.0	2304.5 ± 212.7	↓ 0.1	↑ 17.0
Untreated	1858.1 ± 42.1	1268.3 ± 110.0	1500.8 ± 138.2	↓ 31.8	↓ 19.2
Minoxidil	2024.0 ± 52.9	1880.4 ± 72.5**	2012.8 ± 29.6**	↓ 0.07	↓ 0.0
EA extract	1985.6 ± 51.8	1872.9 ± 52.8**	2095.0 ± 32.8**	↓ 5.7	↑ 5.6
LED	1811.0 ± 55.3	1481.2 ± 81.8	1852.3 ± 82.8*	↓ 18.2	↑ 2.3
Combination	1851.8 ± 73.9	1672.3 ± 137.8*	2115.1 ± 98.5**	↓ 9.7	↑ 14.2

*$p < 0.05$, **$p < 0.01$ compared to the untreated group.

The minoxidil-treated group demonstrated a statistically significant preservation of follicle numbers, particularly evident at Day 35 ($p = 0.000$), consistent with its established pharmacological role in promoting hair regrowth. Similarly, groups treated with EA extract or LED irradiation showed positive effects, with follicle counts increasing by 5.6% and 2.3%, respectively, compared to baseline. These improvements were statistically significant relative to the untreated group ($p = 0.000$ and $p = 0.018$, respectively), indicating that both interventions may mitigate testosterone-induced follicular damage. Notably, the combination treatment group (EA extract and LED irradiation) exhibited the most pronounced recovery, with a 14.2% increase in follicle count by Day 35 compared to Day 0.

3.3. Histological analysis

The physiology group exhibited a predominance of anagen follicles, with a high anagen/telogen ratio (3.0 ± 0.7), reflecting normal hair cycle dynamics. In contrast, the untreated group showed a shift toward follicular regression, characterized by a predominance of telogen follicles, which was approximately 1.9-fold higher than that observed in the physiology group (Table 2). Additionally, a substantial reduction in anagen follicles was noted, resulting in a significantly lower anagen/telogen ratio (0.4 ± 0.2), indicative of impaired hair cycle progression. Treatment with minoxidil moderately increased the total follicle count (153.2 ± 50.0) and substantially reduced the number of telogen follicles compared to the untreated group, resulting in an improved anagen/telogen ratio (2.2 ± 0.8, $p = 0.047$).

Similarly, the EA extract group exhibited a reduction in telogen-phase follicles (5.8 ± 1.9) and an anagen/telogen ratio of 3.3 ± 1.2, indicating a shift toward anagen-dominant cycling and suggesting potential activity in supporting hair-cycle progression. Notably, the LED treatment group demonstrated a pronounced stimulatory effect on hair follicle activity, as evidenced by a significant increase in both total and anagen follicles. LED irradiation was associated with a 1.5-fold increase in total follicle count, together with a higher proportion of follicles in the anagen phase. This resulted in an anagen/telogen ratio of 5.2 ± 1.0, indicating a shift toward anagen-dominant cycling within the treated skin.

The combination group exhibited significantly superior outcomes compared to all other treatment groups, with a total follicle count of 234.5 ± 31.6 and an anagen follicle count of 183.3 ± 31.4, representing approximately a 1.8-fold increase relative to the physiology group. Importantly, these enhancements were achieved without a concomitant rise in telogen follicle numbers, resulting in the highest anagen/telogen ratio of 7.4 ± 2.0, which was statistically significant ($p = 0.006$) compared to the untreated group. Histological analysis suggested more favorable dermal and follicular features in the combination group compared with EA extract or LED alone (Figure 6).

Table 2. Microscopic analysis of the experimental groups at the end of the experiments**.**

Groups	Total	Anagen	Telogen	Anagen/Telogen ratio
Physiology	134.0 ± 31.4	93.0 ± 31.5	26.3 ± 5.3	3.0 ± 0.7
Untreated	100.0 ± 18.3	26.0 ± 10.8	49.7 ± 11.0	0.4 ± 0.2
Minoxidil	153.2 ± 50.0	33.00 ± 16.7	15.8 ± 4.8*	2.2 ± 0.8*
EA extract	165.2 ± 36.0	28.5 ± 15.4	5.8 ± 1.9*	3.3 ± 1.2*
LED	197.3 ± 21.7**	146.5 ± 20.5*	32.9 ± 4.6	5.2 ± 1.0*
Combination	234.5 ± 31.6**	183.3 ± 31.4 *	29.7 ± 4.3	7.4 ± 2.0*

*$p < 0.05$, **$p < 0.01$ compared to the untreated group.

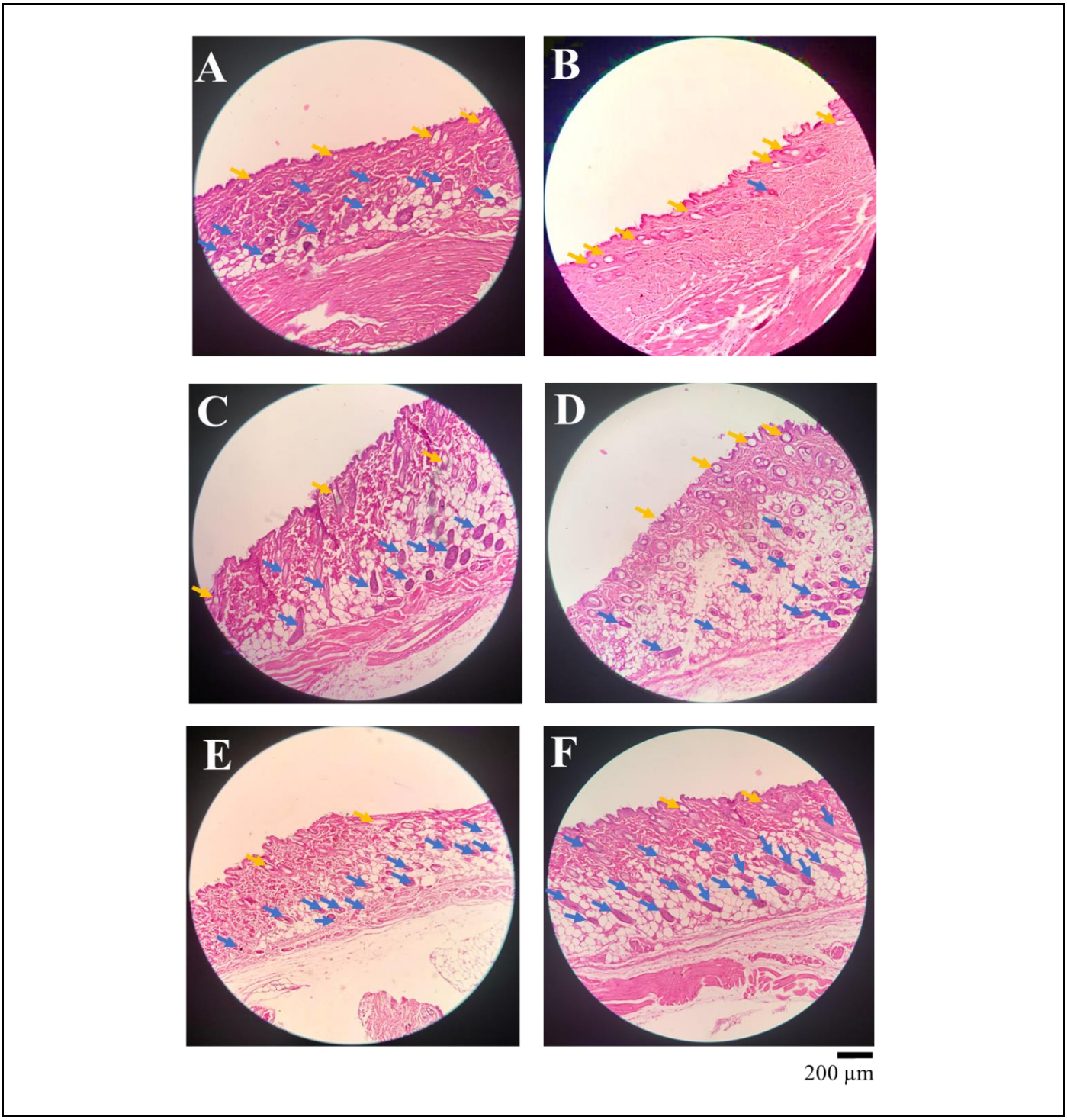

Figure 6. Histological evaluation of hair follicles from the experimental groups. Representative H&E-stained skin sections (10x magnification; scale bar = 200 µm) from the (A) physiology, (B) untreated, (C) minoxidil, (D) EA extract, (E) LED irradiation, and (F) combination-treated groups at the end of the experiment, illustrating differences in hair follicle morphology and hair-cycle distribution. Blue arrows indicate anagen-phase hair follicles, while yellow arrows indicate telogen-phase hair follicles.

4. DISCUSSION

AGA is primarily driven by elevated levels of dihydrotestosterone (DHT), a potent androgen converted from testosterone via 5α-reductase type II at the hair follicle site [4,21]. DHT binds to androgen receptors in dermal papilla cells, leading to shortening of the anagen phase and prolongation of the telogen phase, ultimately resulting in follicular miniaturization and progressive hair thinning. These mechanisms underpin widely used androgen-induced mouse models of hair loss and the pharmacologic validation of anti-androgen strategies.

In this study, subcutaneous testosterone (1 mg/day, 5 days/week for 35 days) in Swiss *albino* mice elicited a hair-loss phenotype consistent with

established androgen-induced AGA paradigms, including reduced follicle counts and a shift toward telogen on histology. This aligns with prior reports showing that exogenous androgens (testosterone or DHT) recapitulate hallmark features of AGA and provide a responsive platform for testing anti-androgenic or pro-regrowth interventions [10,22].

We selected Swiss *albino* mice based on both scientific and practical considerations. Previous studies have demonstrated that Swiss *albino* mice are suitable for investigating hair-follicle growth dynamics and alopecia-related changes, including testosterone-induced hair loss and photobiomodulation-associated hair regrowth, confirming their applicability in alopecia research [14,23,24]. Compared with C57BL/6, whose synchronized hair cycle and pigmentation changes are advantageous for staging but can markedly interfere with optical and photographic assessments due to melanin-related signal attenuation, the unpigmented Swiss *albino* background provides more consistent macroscopic scoring. Additionally, Swiss *albino* mice are the strain routinely available and maintained in our institutional animal facility, ensuring standardized husbandry and experimental conditions throughout the study.

The present study evaluated the effects of Perilla extract, LED irradiation, and their combination on hair regrowth using macroscopic scoring, follicle profiling, and histological assessment. Across these endpoints, each treatment produced measurable changes in hair-follicle characteristics in the testosterone-induced AGA model, and the combination group showed the greatest overall magnitude of response. These findings indicate that all treatment conditions influenced hair cycle-related parameters under the experimental conditions tested.

The leaf extract of *Perilla frutescens* contains several bioactive compounds, notably rosmarinic acid, luteolin, and catechins [7,8]. Among these, rosmarinic acid is the predominant constituent in Perilla extract and has been reported to suppress the activity of testosterone and DHT, inhibit 5α-reductase, and activate the Wnt/β-catenin signaling pathway. This pathway plays a critical role in initiating hair regrowth by promoting the proliferation and migration of hair follicle cells [9,11,25,26.] In our experiment, treatment with EA extract effectively prolonged the anagen phase and significantly reduced the number of telogen follicles, resulting in an anagen/telogen ratio comparable to that of the physiology group. These findings are consistent with previous *in vivo* and *ex vivo* studies demonstrating the capacity of Perilla extract to enhance follicular proliferation and differentiation [9-11].

LLLT, including LED photobiomodulation, has been widely investigated for its regenerative effects on skin and hair follicles. Its proposed mechanisms of action involve enhanced mitochondrial ATP production, modulation of reactive oxygen species, and activation of transcription factors such as NF-κB and HIF-1 [27]. These molecular events collectively promote gene transcription and protein synthesis, which in turn contribute to the activation of the Wnt/β-catenin signaling, a key pathway in hair follicle proliferation and growth [27-29.] In this study, 655 ± 5 nm LED irradiation (2.5 J/cm^2, applied every other day for 20 minutes) resulted in a 1.5-fold increase in total follicle count and a marked rise in anagen-phase follicles, without affecting telogen follicle counts. These findings align with previous reports showing that the wavelength light of 655 ± 5 nm upregulates the expression of β-catenin in the hair matrix. This activation consequently prolongs the anagen phase, accelerates hair shaft elongation and supports the efficacy of photobiomodulation in hair follicle regeneration [15,18,28].

The LED system employed in this study was custom-engineered to enable precise regulation of irradiation parameters. The device integrated an ESP32 microcontroller, a MOSFET switching module, and an LCD interface, facilitating real-time monitoring and control of operational variables. Its structural configuration was optimized to ensure uniform light distribution across four independent treatment compartments, thereby minimizing inter-sample variability and enhancing irradiance consistency. This level of technical precision likely contributed to the reproducibility and therapeutic efficacy observed.

The biological effects of photobiomodulation are critically dependent on irradiance (W/cm²) and exposure duration [30]. Suboptimal irradiance or insufficient exposure time may fail to induce a stimulatory response, whereas excessive irradiance or prolonged illumination can result in inhibitory effects [27]. Thus, achieving an optimal balance between power density and exposure time is essential for therapeutic success. In this study, continuous 20-minute irradiation was not feasible. During LED device testing, heat accumulation was detected on the aluminum structural components, making uninterrupted operation unstable under prolonged use. To address these thermal constraints, an intermittent irradiation protocol was implemented: each session consisted of 10 minutes of exposure followed by a 5-minute rest, then another 10 minutes of exposure, with a 15-minute rest interval preceding subsequent sessions. This approach was adopted to minimize heat buildup while ensuring consistent energy delivery and maintaining treatment efficacy.

The group receiving the combined administration of Perilla extract and LED irradiation exhibited a more pronounced improvement in hair-regrowth parameters compared with each intervention alone. Total follicle counts and the number of anagen-phase follicles increased approximately 1.8-

fold compared to the physiology group. Histological observations further suggested qualitative improvements in overall skin architecture, characterized by more favorable dermal features and enhanced follicular organization, which may contribute to a supportive microenvironment for follicle regeneration. Importantly, these changes occurred without an accompanying increase in telogen-phase follicles, suggesting a shift toward anagen-dominant cycling in the combination group under the conditions tested, without evidence of premature regression.

Collectively, these findings suggest that combining topical EA extract of *Perilla frutescens* with LED photobiomodulation may enhance both macroscopic hair fiber proliferation and microscopic follicular development. This combined approach presents a promising, non-invasive alternative to conventional therapies, particularly for individuals who are unresponsive or intolerant to minoxidil or finasteride. Future research should prioritize the optimization of local pharmaceutical formulations of EA extract and the refinement of LED irradiation parameters to enhance therapeutic efficacy. Furthermore, comprehensive long-term evaluations and translational studies in human populations are essential to determine the clinical applicability and safety of this combined treatment strategy.

5. CONCLUSIONS

In conclusion, this study demonstrates that ethyl acetate extract from *Perilla frutescens* leaves enhances visible hair growth, while LED photobiomodulation promotes follicular transition into the anagen phase. When given together, the two interventions yielded a greater improvement in hair-regrowth outcomes than either treatment alone, including a clear increase in the anagen/telogen ratio relative to physiological controls. These findings provide preliminary *in vivo* evidence that integrating a topical herbal extract with photobiomodulation may offer a complementary strategy for promoting hair regeneration.

6. ACKNOWLEDGEMENTS

We sincerely thank the Department of Pharmacology, School of Pharmacy, University of Medicine and Pharmacy at Ho Chi Minh City, Viet Nam for their valuable support in facilitating this research.

Author contribution

Conceptualization: NT-H and TTH-P. Study design and methods: NT-H and TTH-P. Experiment performance and data collection: NAT-L, DHV-N and TG-T. Data analysis and interpretation: DHV-N and NT-H. Supervision: NT-H. Manuscript drafting and revision: all authors. All authors read and agreed to the final manuscript.

Funding

This study was not funded by any organizations.

Conflict of interest (If any)

All authors declare no competing interest.

Ethics approval

This study protocol was reviewed and approved by the Animal Ethics Committee in Nong Lam University (AEC-NLU), Ho Chi Minh City, Viet Nam under Approval No. NLU-221202, dated October 30, 2022. All procedures complied with relevant institutional and national regulations. The principles of the 3Rs – Replacement, Reduction, and Refinement – were strictly applied to minimize animal use and suffering. Furthermore, this study adhered to the ARRIVE Guidelines 2.0 to ensure transparent and reproducible reporting.

Article info:

Received January 12, 2026
Received in revise form March 25, 2026
Accepted March 29, 2026

REFERENCES

1. Tosti A, Camaeho-Martinez F, Dawber R. Management of androgenetic alopecia. J Eur Acad Dermatol Venereol. 1999;12(3):205-14.
2. Chen S, Li L, Ding W, Zhu Y, Zhou N. Androgenetic alopecia: an update on pathogenesis and pharmacological treatment. Drug Des Devel Ther. 2025;19:7349-63.
3. Otberg N, Finner AM, Shapiro J. Androgenetic alopecia. Endocrinol Metab Clin North Am. 2007;36(2):379-98.
4. Cotsarelis G, Millar SE. Towards a molecular understanding of hair loss and its treatment. Trends Mol Med. 2001;7(7):293-301.
5. Phillips TG, Slomiany WP, Allison R. Hair loss: common causes and treatment. Am Fam Physician. 2017;96(6):371-8.
6. Rogers NE, Avram MR. Medical treatments for male and female pattern hair loss. J Am Acad Dermatol. 2008;59(4):547-66.
7. Hou T, Netala VR, Zhang H, Xing Y, Li H, Zhang Z. *Perilla frutescens*: A rich source of pharmacological active compounds. Molecules. 2022;27(11):3578. doi: 10.3390/molecules27113578.
8. Singh S, Singh S, Kumar S, Verma S. Biological activities and therapeutic potential of *Perilla frutescens* (purple mint): A review. Int J Pharm Sci Res. 2022;13:645-53.
9. Li JJ, Li Z, Gu LJ, Choi KJ, Kim DS, Kim HK, et al. The promotion of hair regrowth by topical application of a *Perilla frutescens* extract through increased cell viability and antagonism of testosterone and dihydrotestosterone. J Nat Med. 2018;72(1):96-105.
10. Giang TT, Trinh NH. Hair growth promoting effect of cream from *Perilla frutescens* leaf extract in cyclophosphamide-induced hair loss in mice. CTUMP Journal. 2019;549-55.
11. Muangsanguan A, Ruksiriwanich W, Linsaenkart P, Tangjaidee P, Sringarm K, Arjin C, et al. Germination enhances phytochemical profiles of Perilla seeds and promotes hair

growth via 5α-reductase inhibition and growth factor pathways. Biology. 2025;14(7):889. doi: 10.3390/biology14070889.
12. Yoon JS, Ku WY, Lee JH, Ahn HC. Low-level light therapy using a helmet-type device for the treatment of androgenetic alopecia: A 16-week, multicenter, randomized, double-blind, sham device-controlled trial. Medicine . 2020;99(29):e21181.
13. Avci P, Gupta A, Sadasivam M, Vecchio D, Pam Z, Pam N, et al. Low-Level Laser (Light) Therapy (LLLT) in skin: stimulating, healing, restoring. Semin Cutan Med Surg. 2013;32:41-52.
14. Shukla S, Sahu K, Verma Y, Rao K, Dube A, Gupta P. Effect of helium-neon laser irradiation on hair follicle growth cycle of Swiss albino mice. Skin Pharmacol Physiol. 2010;23(2):79-85.
15. Yang K, Tang Y, Ma Y, Liu Q, Huang Y, Zhang Y, et al. Hair growth promoting effects of 650 nm red light stimulation on human hair follicles and study of its mechanisms via RNA sequencing transcriptome analysis. Ann Dermatol. 2021;33(6):553.
16. Heiskanen V, Hamblin MR. Photobiomodulation: lasers vs. light emitting diodes? Photochem Photobiol Sci. 2018;17(8):1003-17.
17. Wikramanayake TC, Rodriguez RAR, Choudhary S, Mauro LM, Nouri K, Schachner LA, et al. Effects of the Lexington LaserComb on hair regrowth in the C3H/HeJ mouse model of alopecia areata. Lasers Med Sci. 2012;27:431-6.
18. Joo HJ, Jeong KH, Kim JE, Kang H. Various wavelengths of light-emitting diode light regulate the proliferation of human dermal papilla cells and hair follicles via Wnt/β-catenin and the extracellular signal-regulated kinase pathways. Ann Dermatol. 2017;29(6):747-54.
19. Welle M. Basic principles of hair follicle structure, morphogenesis, and regeneration. Veterinary pathology. 2023;60(6):732-47.
20. El-Domyati M, Hosam W, Moftah NH, Abdel Raouf H, Saad SM. Hair follicle changes following intense pulsed light axillary hair reduction: histometrical, histological and immunohistochemical evaluation. Arch Dermatol Res. 2017;309(3):191-202.
21. Trüeb RM. Molecular mechanisms of androgenetic alopecia. Exp Gerontol. 2002;37(8-9):981-90.
22. Noubarani M, Rostamkhani H, Erfan M, Kamalinejad M, Eskandari MR, Babaeian M, et al. Effect of adiantum *Capillus veneris* Linn on an animal model of testosterone-induced hair loss. Iran J Pharm Res. 2014;13(Suppl):113-8.
23. Jawarkari D, Vyas JV, Paithankar VV, Wankhade A. Hair growth promoting activity of helianthus annuus in testosterone induced alopecia in mice model. Int J Pharm Sci Med. 2023;8:80-91. doi: 10.47760/ijpsm.2023.v08i05.011.
24. Kusumawardani A, Mulianto N, Nareswari A, Monica PW, Oktaviani T. Testosterone-induced androgenetic alopecia mice model: A preliminary study. Int J App Pharm. 2025;17(2):78-82. doi: 10.22159/ijap.2025.v17s2.09.
25. Soe ZC, Ei ZZ, Visuttijai K, Chanvorachote P. Potential natural products regulation of molecular signaling pathway in dermal papilla stem cells. Molecules. 2023;28(14):5517.
26. Mehta A, Motavaf M, Raza D, McLure AJ, Osei-Opare KD, Bordone LA, et al. Revolutionary approaches to hair regrowth: follicle neogenesis, Wnt/ß-catenin signaling, and emerging therapies. Cells.2025;14(11). doi: 10.3390/cells14110779.
27. Pillai JK, Mysore V. Role of low-level light therapy (LLLT) in androgenetic alopecia. J Cutan Aesthet Surg. 2021;14(4):385-91.
28. Han L, Liu B, Chen X, Chen H, Deng W, Yang C, et al. Activation of Wnt/β-catenin signaling is involved in hair growth-promoting effect of 655-nm red light and LED in *in vitro* culture model. Lasers Med Sci. 2018;33(3):637-45.
29. Jin H, Zou Z, Chang H, Shen Q, Liu L, Xing D. Photobiomodulation therapy for hair regeneration: A synergetic activation of β-CATENIN in hair follicle stem cells by ROS and paracrine WNTs. Stem cell reports. 2021;16(6):1568-83. doi: 10.1016/j.stemcr.2021.04.015.
30. Chung H, Dai T, Sharma SK, Huang Y-Y, Carroll JD, Hamblin MR. The nuts and bolts of low-level laser (light) therapy. Ann Biomed Eng. 2012;40(2):516-33.